World Electric Vehicle Journal

MDPI

Article

Sizing a Renewable-Based Microgrid to Supply an Electric Vehicle Charging Station: A Design and Modelling Approach

Amirhossein Khazali [1,*], Yazan Al-Wreikat [1], Ewan J. Fraser [1], Mobin Naderi [2], Matthew J. Smith [2], Suleiman M. Sharkh [1], Richard G. Wills [1], Daniel T. Gladwin [2], David A. Stone [2] and Andrew J. Cruden [1]

[1] School of Engineering, University of Southampton, Southampton SO17 1BJ, UK; y.m.y.al-wreikat@soton.ac.uk (Y.A.-W.); e.j.fraser@soton.ac.uk (E.J.F.); s.m.sharkh@soton.ac.uk (S.M.S.); rgaw@soton.ac.uk (R.G.W.); a.j.cruden@soton.ac.uk (A.J.C.)

[2] Department of Electronic and Electrical Engineering, University of Sheffield, Sheffield S10 2TN, UK; m.naderi@sheffield.ac.uk (M.N.); matt.j.smith@sheffield.ac.uk (M.J.S.); d.gladwin@sheffield.ac.uk (D.T.G.); d.a.stone@sheffield.ac.uk (D.A.S.)

* Correspondence: a.khazali@soton.ac.uk

Abstract: In this paper, an optimisation framework is presented for planning a stand-alone microgrid for supplying EV charging (EVC) stations as a design and modelling approach for the FEVER (future electric vehicle energy networks supporting renewables) project. The main problem of the microgrid capacity sizing is making a compromise between the planning cost and providing the EV charging load with a renewable generation-based system. Hence, obtaining the optimal capacity for the microgrid components in order to acquire the desired level of reliability at minimum cost can be challenging. The proposed planning scheme specifies the size of the renewable generation and battery energy storage systems not only to maintain the generation–load balance but also to minimise the capital cost (CAPEX) and operational expenditures (OPEX). To study the impact of renewable generation and EV charging uncertainties, the information gap decision theory (IGDT) is used to include risk-averse (RA) and opportunity-seeking (OS) strategies in the planning optimisation framework. The simulations indicate that the planning scheme can acquire the global optimal solution for the capacity of each element and for a certain level of reliability or obtain the global optimal level of reliability in addition to the capacities to maximise the net present value (NPV) of the system. The total planning cost changes in the range of GBP 79,773 to GBP 131,428 when the expected energy not supplied (EENS) changes in the interval of 10 to 1%. The optimiser plans PV generation systems in the interval of 50 to 63 kW and battery energy storage system in the interval of 130 to 280 kWh and with trivial capacities of wind turbine generation. The results also show that by increasing the total cost according to an uncertainty budget, the uncertainties caused by EV charging load and PV generation can be managed according to a robustness radius. Furthermore, by adopting an opportunity-seeking strategy, the total planning cost can be decreased proportional to the variations in these uncertain parameters within an opportuneness radius.

Keywords: microgrid; renewable energy; battery energy storage system; optimisation; information gap decision theory (IGDT)

Citation: Khazali, A.; Al-Wreikat, Y.; Fraser, E.J.; Naderi, M.; Smith, M.J.; Sharkh, S.M.; Wills, R.G.; Gladwin, D.T.; Stone, D.A.; Cruden, A.J. Sizing a Renewable-Based Microgrid to Supply an Electric Vehicle Charging Station: A Design and Modelling Approach. *World Electr. Veh. J.* **2024**, *15*, 363. https://doi.org/10.3390/wevj15080363

Academic Editor: Ghanim A. Putrus

Received: 3 July 2024
Revised: 24 July 2024
Accepted: 8 August 2024
Published: 12 August 2024

1. Introduction

The interest in reducing carbon emissions generated by fossil fuels has resulted in the adoption of new development strategies in the energy and transportation sector. While in the former this strategy is based on increasing the penetration of renewable energy sources (RES) in power grids, the latter pursues increasing electrification of the transportation sector [1]. These policies, coupled with a generally congested National Grid, have led to significant interest in establishing carbon-free microgrids for charging electric vehicles. However, sizing renewable sources to supply EVC stations can be challenging. On one hand, a system can be oversized, and additional costs can be incurred by the stakeholders'

oversizing of renewable energy sources (RESs). On the other hand, if the capacities of these elements are underestimated, it results in a system that cannot provide adequate energy to the EVC station [2]. Hence, appropriate optimisation frameworks must be developed to determine the best capacity for each element [3,4].

The capacity sizing problem of microgrids has been investigated by several researchers. In [5], Bandyopadhyay et al. present a techno-economic framework for obtaining the optimal size of photovoltaic (PV) generation systems and BESS capacities in a microgrid. In the paper, they study the effect of the geographical location of the microgrid on capacity sizing of these components.

A stand-alone system composed of wind turbines (WTs), a PV system, and a battery energy storage system (BESS) is sized in [6], incorporating demand-side management. The results indicate that for various combinations, the plan composed of WTs, a PV system, and BESS is the best plan from the economic point of view. Particle swarm optimization (PSO) is used in this paper; however, reaching the global optimal point cannot be guaranteed by this approach.

An analytical sizing approach is introduced in [7] for sizing the capacity of vanadium redox batteries for microgrid systems. The nonlinear efficiencies and operating characteristics are considered in this study. The microgrid, nonetheless, is not off-grid and the optimisation problem is solved by dynamic programming. Planning of isolated BESSs for isolated microgrids is studied in [8]. Alharbi et al. solve a two-stage mixed integer linear programming (MILP) formulation where, in the first stage, the capacity of the battery is specified, and the second stage determines the installation year of the battery, but the microgrid is not renewable-based. In addition, the reliability of the system is not adjustable for it. An analytical approach for sizing BESS in microgrids is presented in [9] with the aim of minimising the unused capacity of the BESS and maximising renewable consumption. The results indicate that the solution ensures that there is no wasted energy storage capacity and shows how energy leakage affects the sizing of long-term storage. Nevertheless, Ref. [9] does not regard the net present value of the system. Battery degradation is studied in [10] for microgrid optimal planning to increase the precision and economic feasibility of the microgrid capacity sizing problem. Degradation of lithium-ion batteries for another capacity planning problem is also studied in [11] where a new battery degradation model is presented for microgrid planning. The amount of unmet load is controlled by the value of loss load included in the objective function for this method. A stochastic programming approach is presented in [12] where Habib et al. include smart prosumers and electric vehicles in the microgrid planning problem. Multi-dimensional uncertainties are used in [13] for the microgrid capacity planning problem. Chen et al. use a novel technique for generating scenarios which are similar to the real data, but the planning is not for a renewable-based system. Also, there is no possibility for adjusting the unmet load in [13].

The integration of electric vehicle charging stations in energy grids has also been studied in several papers. For instance, the integrated planning of electricity networks and fast charging stations is studied in [14]. The planning scheme is based on the cost of the system and the quality of service to the customers. Plug-in electric vehicle load modelling is presented in [15] for charging scheduling strategies. This modelling is used in smart charging algorithms and to increase the knowledge of future behaviours to aid charging scheduling. A load modelling scheme is presented in [16] for electric-vehicle fast charging stations. The method utilises the measured data and an iterative optimisation approach to acquire an accurate load model for these stations. An optimal EV charging station planning scheme based on EV load forecasting is studied in [17] where the spatial-temporal EV load is forecasted according to the road topology.

Specifying the level of uncertainty for decision-making problems with stochastic parameters is challenging. While considering high levels of uncertainty increases the operation cost, underestimating the uncertainty level of the system results in decreasing the robustness of the plan [18]. On the other hand, accurate statistical data are used for evaluating the uncertain space of the problem, which is not always available. The

information gap decision theory (IGDT) approach is an uncertainty management approach that is suitable for problems which deal with the scarcity of data and can provide solutions for various levels of robustness (or opportunity-seeking levels) [19]. IGDT has been used in several types of research for microgrid operation and planning [20]. In [21] the IGDT approach is used for operating a microgrid with liquid air energy storage; in this research, the capacity of microgrid elements is pre-specified but microgrid capacity planning is not considered. In [22], IGDT is used for microgrid planning for e-mobility infrastructure; however, in this research, the IGDT is only used for managing the uncertainty caused by EV charging load. In [23], the author uses IGDT for operating a combined cooling, heat, and power microgrid; this study also focuses on microgrid operation and only takes the load uncertainty into account. Also, in [24] a similar uncertainty management scheme is used for capacity planning; however, the research does not mention how the renewable generation uncertainty is harnessed by this approach.

In this paper, a reliability-constrained optimisation model is presented for sizing renewable generation systems and battery energy storage systems within EVC stations at a visitor attraction site near Southampton, UK. In this paper, reliability refers to the proportion of EV charging load that is met by the system during the planning horizon. The main contribution of this research is presenting a MILP formulation where the decision maker can adapt the desired plan according to the reliability level of the system for electric vehicle charging stations. Two scenarios are investigated, with and without reliability constraints, to quantify and demonstrate their significance. In addition, a linear model is presented for utilising IGDT for managing uncertainties caused by EV charging demand and renewable generation.

The next section of this paper is dedicated to explaining the structure of the problem. The third section presents the microgrid capacity planning formulation. Simulation results are presented in Section 4. Section 5 concludes the paper.

2. Stand-Alone Microgrid Planning

In this section, the proposed model for the microgrid planning is illustrated. Figure 1 shows the structure of the microgrid which is composed of wind turbines, PV panels, batteries, and the EV charging stations all connected to a common busbar with power electronic interfaces. It is worth mentioning that other miscellaneous loads can also be supplied by this system. In this system, the EVC stations are supplied by PV generation and wind turbines. When there is a surplus of energy, the excess is used to charge the BESS. If the battery state of charge (SOC) is greater than a specified level, the excess energy will be curtailed. Conversely, when there is a shortage of renewable energy production, the battery will discharge to supply the EVC stations. If the battery SOC falls beneath a specified value, load shedding is inevitable. It is the case that PV panels and wind turbines are interruptible and volatile generation sources, and their generation depends on the geographical location of the system. Also, it is true that battery energy storage systems have a more deterministic behaviour, and they can be scheduled if they do not reach the state of charge limitations. However, these components complement each other, and their performance should not be considered separately. Without the renewables, the batteries cannot be charged, and without the batteries, the generation of the renewables is not manageable.

Two scenarios are investigated. In the first scenario, the maximum amount of unmet load is constrained. In the second scenario, a cost–benefit model is formulated where the income acquired by charging EVs is included in the objective function, but without reliability constraints. Figure 2 shows an overview of the optimisation planning problem of a microgrid including the objective function elements, constraints, and decision variables. As illustrated, the objective function consists of the CAPEX and OPEX of various components of the system.

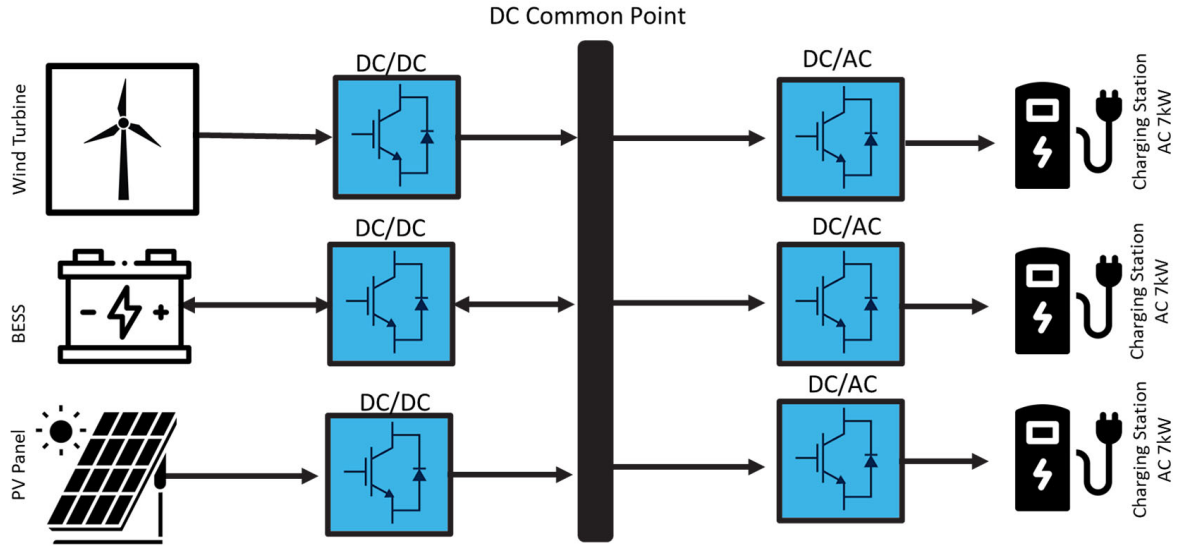

Figure 1. Structure of the stand-alone microgrid.

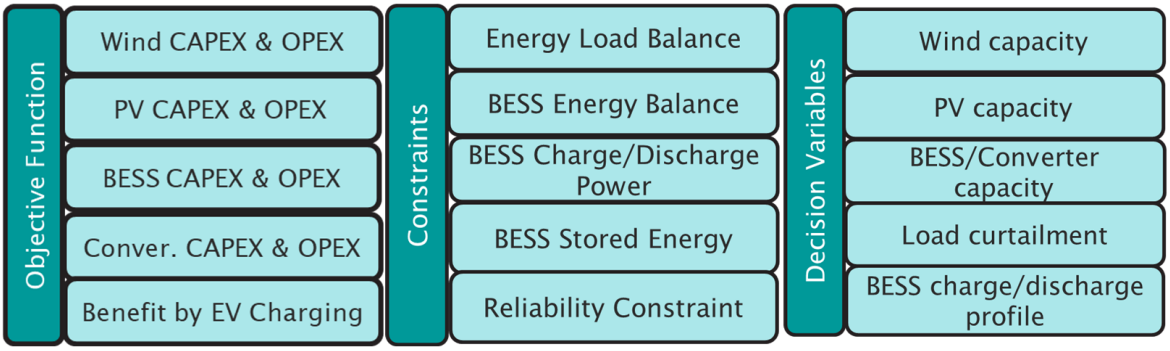

Figure 2. Overview of the optimisation problem.

The respective mathematical formulations of the two scenarios are presented in the next section.

3. Mathematical Formulation

3.1. Scenario1: Unmet Load Reliability Constrained Model

In this section, the microgrid capacity planning scheme for reliability-constrained formulation is presented. The objective function for this study case is defined in (1). This relation is composed of the total CAPEX and OPEX. The CAPEX and OPEX for each element of the microgrid are calculated using the following equations:

$$MinOF = CAPEX + OPEX \tag{1}$$

$$CAPEX = CAPEX_W C_W + CAPEX_{PV} C_{PV} + CAPEX_{BESS} C_{BESS} + CAPEX_{Conv} C_{Conv} \tag{2}$$

$$OPEX = OPEX_W + OPEX_{PV} + OPEX_{BESS} + OPEX_{Conv} \tag{3}$$

$$OPEX_W = \sum_{y=1}^{N_Y} \sum_{t=1}^{N_T} (OPEX_{W,F} C_W + OPEX_{W,V} C_W Wind(y,t) \Delta t) \tag{4}$$

$$OPEX_{PV} = \sum_{y=1}^{N_Y} \sum_{t=1}^{N_T} (OPEX_{PV,F} C_{PV} + OPEX_{PV,V} C_{PV} PV(y,t) \Delta t) \tag{5}$$

$$OPEX_{BESS} = \sum_{y=1}^{N_Y} \sum_{t=1}^{N_T} OPEX_{BESS,F} C_{ConV} + OPEX_{BESS,V}(P_{ch}(y,t) + P_{dis}(y,t))\Delta t \quad (6)$$

The capacity of each of the microgrid elements is restricted by the following relations:

$$C_{PV} \leq C_{PV,max} \quad (7)$$

$$C_W \leq C_{W,max} \quad (8)$$

$$C_{BESS} \leq C_{BESS,max} \quad (9)$$

$$C_{ConV} \leq C_{ConV,max} \quad (10)$$

It is the case that renewable energy generation systems, especially PV panels, occupy a lot of space and one of their main challenges is finding appropriate sites for their installation. However, the presented model is able to cope with this challenge by the constraints presented in relations (7)–(10). In these relations, the capacity (or number of elements) of each component can be restricted to a maximum value which can be determined by the amount of provided space for installation. By doing so, the optimiser is able to find the capacity size of each element with the least cost while satisfying the capacity constraint.

The energy balance for the system needs to be maintained:

$$C_W Wind(y,t)\Delta t + C_{PV} PV(y,t)\Delta t + P_{dis}(y,t)\Delta t + UL(y,t) = P_{ch}(y,t)\Delta t + EV(y,t) + RS(y,t) \quad (11)$$

In the above equation, the sum of energy produced by renewable sources and the energy discharged by the battery must be equal to the load and the amount of energy charging the battery. In addition, the unsupplied load and renewable spillage terms in (11) are used to make this relation feasible in case of energy shortage or when there is a surplus of energy, respectively.

The operational limitations of the BESS are as follows:

$$P_{ch}(y,t) \leq C_{ConV} \quad (12)$$

$$P_{dis}(y,t) \leq C_{ConV} \quad (13)$$

$$P_{ch}(y,t) \leq M u_{ch}(y,t) \quad (14)$$

$$P_{dis}(y,t) \leq M u_{dis}(y,t) \quad (15)$$

$$u_{ch}(y,t) + u_{dis}(y,t) \leq 1 \quad (16)$$

$$E(y,t) = E(y,t-1) + (\eta_{ch}\eta_{ConV} P_{ch}(t)\Delta t) - (P_{dis}(t)\Delta t / \eta_{dis}\eta_{ConV}) \quad (17)$$

$$SOC_{min} C_{BESS} \leq E(y,t) \leq SOC_{max} C_{BESS} \quad (18)$$

In (12) and (13) the power charged and discharged by the BESS is limited by the converter size. Equations (14)–(16) specify linearised formulations for determining the operation state of the BESS. Relation (17) calculates the stored energy in the BESS for each time of each year, taking the losses in the converters and batteries into account. Finally, the stored energy in the BESS is limited in (18) by the maximum (SOC_{max}) and minimum (SOC_{min}) states of charge.

The reliability constraints of the problem are as follows:

$$EENS(y) = \sum_{t=1}^{N_T} UL(y,t) \quad (19)$$

$$EENS(y) \leq EENS_{max}.\sum_{t=1}^{N_T} EV(y,t) \tag{20}$$

In these relations, (19) calculates the percentage of unmet load for each year and (20) limits this variable to a maximum value $EENS_{max}$ $(0 \leq EENS_{max} \leq 1)$.

3.2. Model 2: Cost–Benefit Scenario without Reliability Constraints

The second scenario includes the benefit acquired by this system for the stakeholders. It is defined by subtracting the objective function defined in (1) from the income acquired by charging electric vehicles and considering the discount factor r as follows:

$$MinOF = CAPEX + \sum_{y=1}^{N_Y} \frac{1}{(1+r)^y}\left(OPEX - \sum_{y=1}^{N_Y} Pr_{EV}(TEV(y) - EENS(y))\right) \tag{21}$$

$$TEV(y) = \sum_{t=1}^{N_T} EV(y,t) \tag{22}$$

In this scenario, the reliability constraint in (20) is not considered, which maximises the obtained profit, specified by the objective function (21). Hence, this scenario uses the objective function (21) and the relations (2)–(19), and (22).

3.3. Information Gap Decision Theory for Optimal Microgrid Capacity Planning

This section presents the formulation using the IGDT approach for managing the uncertainties caused by renewable generation (as will be seen later, the contribution of wind generation is trivial according to the results that will be presented in section four, and therefore only the uncertainty of the PV generation system is considered) and EV charging load. Information gap decision theory is an uncertainty management approach applied to optimisation problems with a high degree of uncertainty. This method specifies for a specific amount of exacerbation of the objective function (in this case increasing the total planning cost), how much the negative effect of the uncertain parameters on the objective function can be intensified (decrease in renewable generation and increase in EV charging load for this case). Therefore, the decision maker can make a risk-averse plan which is robust against the worst assumed scenario defined in terms of variations in uncertain parameters according to an uncertainty radius. Conversely, for the opportuneness strategy, the decision maker is optimistic about the uncertain parameters. This strategy calculates for a certain amount of improvement in the objective function (decreasing total planning cost for this case), how much should the uncertain parameters improve (decrease for the EV charging load and increase in renewable generation).

Using the envelope-bound information-gap model [25] and assuming a maximum variation in the uncertain parameter proportional to the parameter used for the deterministic model, the uncertain models for EV charging and PV generation can be formulated as (23) and (24).

$$U(\alpha_{EV}, EV) = \left\{ \boldsymbol{EV} : \frac{\left|\hat{EV}(y,t) - EV(y,t)\right|}{EV(y,t)} \leq \alpha_{EV} \right\}, \alpha_{EV} \geq 0 \tag{23}$$

$$U(\alpha_{PV}, PV) = \left\{ \boldsymbol{PV} : \frac{\left|\hat{PV}(y,t) - PV(y,t)\right|}{PV(y,t)} \leq \alpha_{PV} \right\}, \alpha_{PV} \geq 0 \tag{24}$$

In (23) and (24), ***EV*** and ***PV*** show the uncertainty set for the EV charging load and the PV generation system. α_{EV} and α_{PV} show the uncertainty radius for the EV charging load and PV generation systems, respectively. $\hat{EV}$ and $\hat{PV}$ show the uncertain electric vehicle charging load and the uncertain PV generation for each hour of each year. According to the uncertainty sets that are defined for the EV charging load and the PV generation, the decision maker is seeking a solution which is robust against the variations in the uncertain

parameters. The risk-averse strategy for microgrid capacity sizing can be formulated as follows:

$$\hat{\alpha}_{EV}(X, B_C) = max\left\{\alpha_{EV} : \left(max_{\hat{EV}\in U(\alpha_{EV},EV)} OF < OF_D\left(1+\sigma_{EV}^{RA}\right)\right)\right\} \tag{25}$$

where OF_D is the total planning cost for the deterministic case (obtained by solving the model in Section 3.1), and σ_{EV}^{RA} shows the uncertainty budget for the case that the uncertainty caused by the EV charging load is studied.

Relation (25) can be written as a single-level optimisation problem as (26)–(28) and considering relations (2)–(10) and (12)–(20).

$$max\alpha_{EV} \tag{26}$$

$$OF < OF_D\left(1+\sigma_{EV}^{RA}\right) \tag{27}$$

$$\begin{aligned} C_W Wind(y,t)\Delta t + C_{PV} PV(y,t)\Delta t + P_{dis}(y,t)\Delta t + UL(y,t) \\ = P_{ch}(y,t)\Delta t + (1+\alpha_{EV})EV(y,t) + RS(y,t) \end{aligned} \tag{28}$$

The presented optimisation model shows, for an uncertainty budget of σ_{EV}^{RA}, how much the EV charging load can increase without violating any constraints of the main microgrid optimal sizing problem.

Like the EV charging load, for the PV generation, the risk-averse optimisation framework can be formulated as (29)–(31) and considering relations (2)–(10) and (12)–(20).

$$max\alpha_{PV} \tag{29}$$

$$OF < OF_D\left(1+\sigma_{PV}^{RA}\right) \tag{30}$$

$$\begin{aligned} C_W Wind(y,t)\Delta t + C_{PV}(1-\alpha_{PV}).PV(y,t)\Delta t + P_{dis}(y,t)\Delta t + UL(y,t) \\ = P_{ch}(y,t)\Delta t + EV(y,t) + RS(y,t) \end{aligned} \tag{31}$$

Equations (29)–(31) shows, for an uncertainty budget of σ_{PV}^{RA}, how much the PV generation can decrease while all the constraints are still feasible. In (31), there is a nonlinear term caused by the multiplication of two variables ($\alpha_{PV}.C_{PV}$). To linearise this term, a binary expansion scheme is used. To do so, the robustness radius α_{PV} is defined as

$$\alpha_{PV} = \left(\frac{1}{2^{N_z}-1}\right)\sum_{z=0}^{N_z} 2^z \gamma_{RA}(z) \tag{32}$$

In (32), N_z is the total number of binary variables. $\gamma_{RA}(z)$ is the corresponding binary variable of each z. By multiplying C_{PV} and the equivalent relation in (32) for α_{PV}, a nonlinear variable is obtained by the multiplication of the binary variable $\gamma_{RA}(z)$ and C_{PV}. By defining this product of these two nonlinear variables as $\rho_{RA}(z)$, α_{PV}, C_{PV} can be replaced by the following linear relationships:

$$\alpha_{PV}.C_{PV} = \xi_{RA} = \left(\frac{1}{2^{N_z}-1}\right)\sum_{z=0}^{N_z} 2^z \rho_{RA}(z) \tag{33}$$

$$-M\gamma_{RA}(z) \le \rho_{RA}(z) \le M\gamma_{RA}(z) \tag{34}$$

$$-M(1-\gamma_{RA}(z)) + C_{PV} \le \rho_{RA}(z) \le M(1-\gamma_{RA}(z)) + C_{PV} \tag{35}$$

Eventually, in (31), the terms α_{PV}, C_{PV} are replaced by ξ_{RA} and the relations in (33)–(35) are added to the main optimisation problem.

In the second strategy, the decision maker has an optimistic view of the stochastic parameters. The model shows, for a decrease in the planning cost according to an oppor-

tunistic factor of σ_{EV}^{RA}, how much the EV charging load has to decrease according to an opportuneness radius of β_{EV} of the EV charging load. The formulation for this model is as (36)–(38) and considering (2)–(10) and (12)–(20).

$$min\beta_{EV} \tag{36}$$

$$OF < OF_D(1 - \sigma_{EV}^{os}) \tag{37}$$

$$\begin{aligned} C_W Wind(y,t)\Delta t + C_{PV} PV(y,t)\Delta t + P_{dis}(y,t)\Delta t + UL(y,t) \\ = P_{ch}(y,t)\Delta t + (1 - \beta_{EV})EV(y,t) + RS(y,t) \end{aligned} \tag{38}$$

Finally, for an opportuneness radius of β_{PV} and an opportunistic factor of σ_{PV}^{os}, the opportunity-seeking model for the variations in the PV generation system can be formulated as (39)–(41) and regarding relations (2)–(10) and (12)–(20).

$$min\beta_{PV} \tag{39}$$

$$OF < OF_D(1 - \sigma_{PV}^{os}) \tag{40}$$

$$\begin{aligned} C_W Wind(y,t)\Delta t + C_{PV}(1 + \beta_{PV}) PV(y,t)\Delta t + P_{dis}(y,t)\Delta t + UL(y,t) \\ = P_{ch}(y,t)\Delta t + EV(y,t) + RS(y,t) \end{aligned} \tag{41}$$

Similar to the risk-averse strategy formulation, the nonlinear term $C_{PV}\beta_{PV}$ can be linearised according to the following relations:

$$\beta_{PV}.C_{PV} = \xi_{OS} = \left(\frac{1}{2^{N_z} - 1}\right) \sum_{z=0}^{N_z} 2^z \rho_{OS}(z) \tag{42}$$

$$-M\gamma_{OS}(z) \leq \rho_{OS}(z) \leq M\gamma_{OS}(z) \tag{43}$$

$$-M(1 - \gamma_{OS}(z)) + C_{PV} \leq \rho_{OS}(z) \leq M(1 - \gamma_{OS}(z)) + C_{PV} \tag{44}$$

4. Simulation Results

The visitor attraction site of the microgrid has ten chargers, each with a capacity of 7 kW. In this study, 6.2 kW wind turbines and 200 Wp PV panels with an efficiency of 15.6% are used [26]. The wind speed–power curve for the wind turbines is extracted from [27]. The capital costs of the wind turbine and PV panels are 5000 GBP/kW and 730 GBP/kW, respectively [28]. In addition, the ESS uses lithium-ion batteries with a capital cost of 146 GBP/kWh [29] and an efficiency of 97.5%. Finally, the capital cost for the converter is 90 GBP/kW with an efficiency of 95%. The price of each EV charger is GBP 1500, and 10 chargers are installed. The total CDM (construction, design, and management) cost is assumed to be GBP 20,000 and the EV modelling is fulfilled according to [28]. The planning horizon is 10 years, and the total capacity of each technology is installed in the first year. The optimisation problem regards a load profile over a ten-year period. Hence, there will be no concerns about the growth of the EV charging load and there will be no need for upgrading the system. All components are sized and installed at the first operating year to last for ten years. The normalised renewable generation profiles for 1 year are shown in Figure 3 with 30 min resolution. It is worth mentioning that various geographical locations can change the results and the size of each component. Each geographical location has its own solar radiation and wind speed profile for each year. These parameters change the power generated by PV panels and wind turbines at different times of the year. Accordingly, the size of various elements including the PV panels, wind turbines, and battery energy storage systems change, which results in variations in the total capacity planning costs. The more the geographical locations differ, the greater the change for different geographical coordinates in terms of component sizes and planning costs. The formulation is modelled

as an MILP formulation in Python and solved using the GUROBI solver [30]. The following sub-sections present the results for the two scenarios for the FEVER project [31].

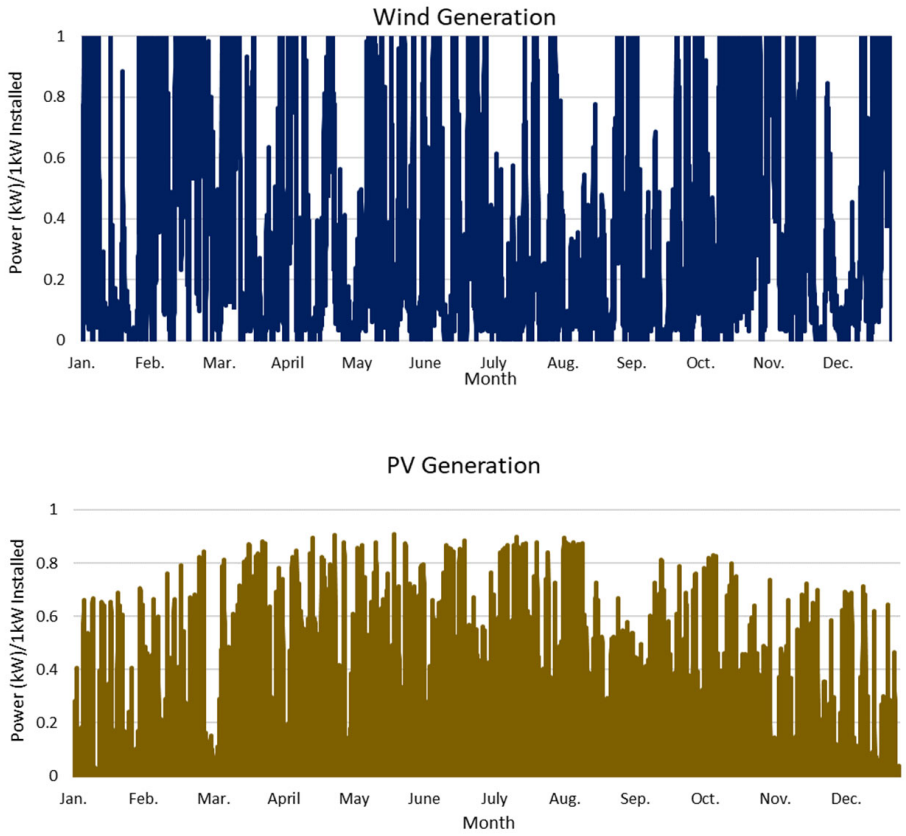

Figure 3. Normalised wind and PV generation profiles for one year (30-min interval).

4.1. Results for the Unmet Load-Constrained Scenario

In this section of the study, the results are presented for a range of EENS from 1% to 10%. Figure 4 indicates the variations in the total and planning cost for each of these reliability levels. In this figure it is observed that for the highest level of reliability, the total cost and planning cost of the system are GBP 131,428 and GBP 116,669, respectively. Conversely, for an EENS of 10% for each year, these costs drop to GBP 79,773 and GBP 68,743, respectively. In addition, in this scenario, the capacity of each element for each level of reliability is shown in Figure 5. In this figure, it is shown that for all levels of reliability, the PV generation capacity fluctuates around 50 kW. When a reliability level more than 97% is desired, nonetheless, this capacity increase to 63 kW (100% reliability). Also, the variation in the BESS capacity shows that for reliability levels from 90 to 97%, the optimiser increases the battery capacity to cope with decreasing the EENS, and for the highest reliability level the BESS capacity increases to 280 kWh. The wind capacity for all levels of reliability is under 6.2 kW, which is less than the capacity of one turbine, and when the level of reliability changes, the variations in the wind generation capacity are trivial. The reason that the required wind generation capacity is so small is not only because of the higher price of wind turbines compared to PV panels but also the load characteristic of the microgrid site. The load for the visitor attraction site is concentrated in the diurnal hours which makes it manageable by PV generation systems and batteries. Hence, instead of sizing expensive wind turbines, the optimiser prefers to use PV generation and BESS to minimise the cost of the system.

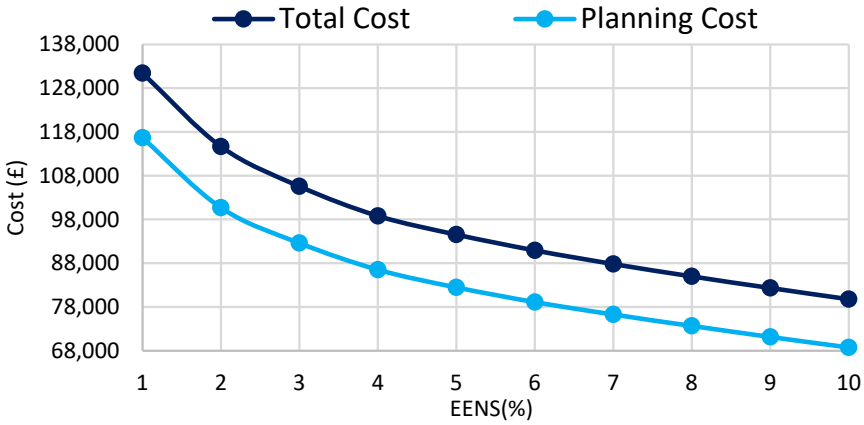

Figure 4. Total cost and planning cost for each level of reliability.

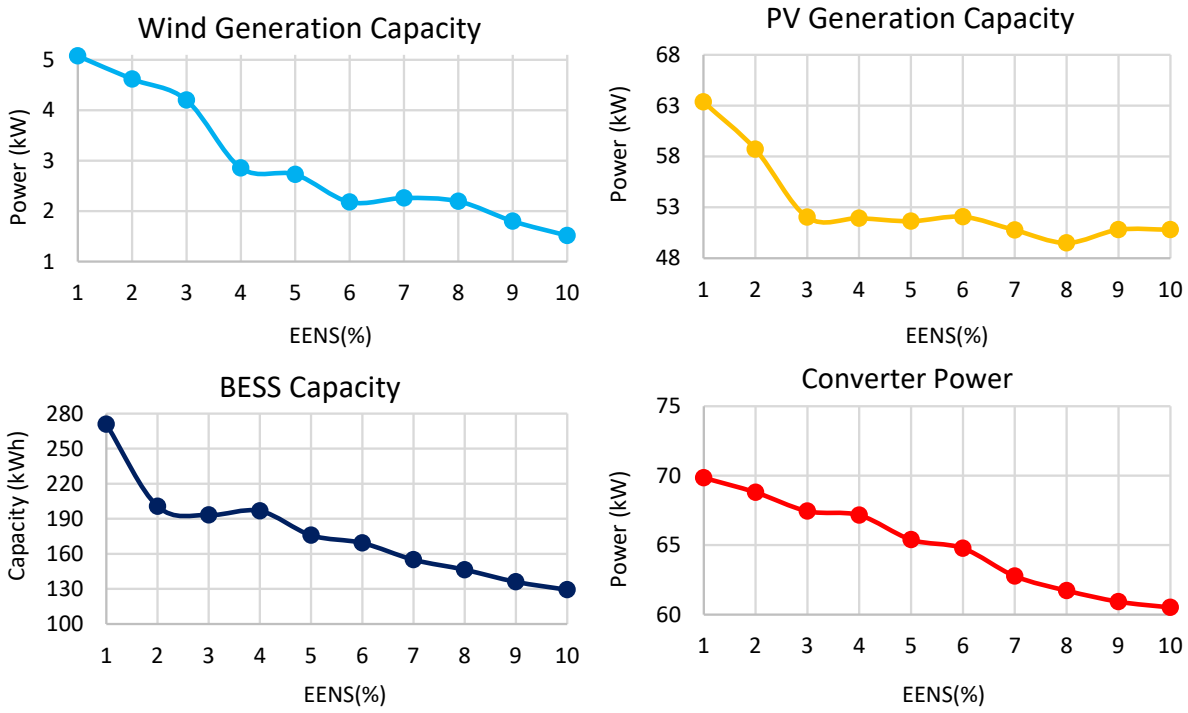

Figure 5. Capacity of each component of the microgrid versus EENS.

For the converter, as the peak load is 70 kW, the size of the converter is near to this value, especially when the EENS is more restricted. It is worth mentioning that if an EENS of 0 is sought after, the total planning cost of the system increases to GBP 265,891 with 233 kW PV and 401 kWh BESS capacity and no wind generation. The size of the converter for this case remains at 70 kW.

For the battery, the charge and discharge profiles are shown in Figure 6 for the last year of the simulation. The total energies charged and discharged when EENS is restricted to 1% are 26,745 kWh and 22,860 kWh, respectively. The stored energy for these two cases is shown in Figure 7.

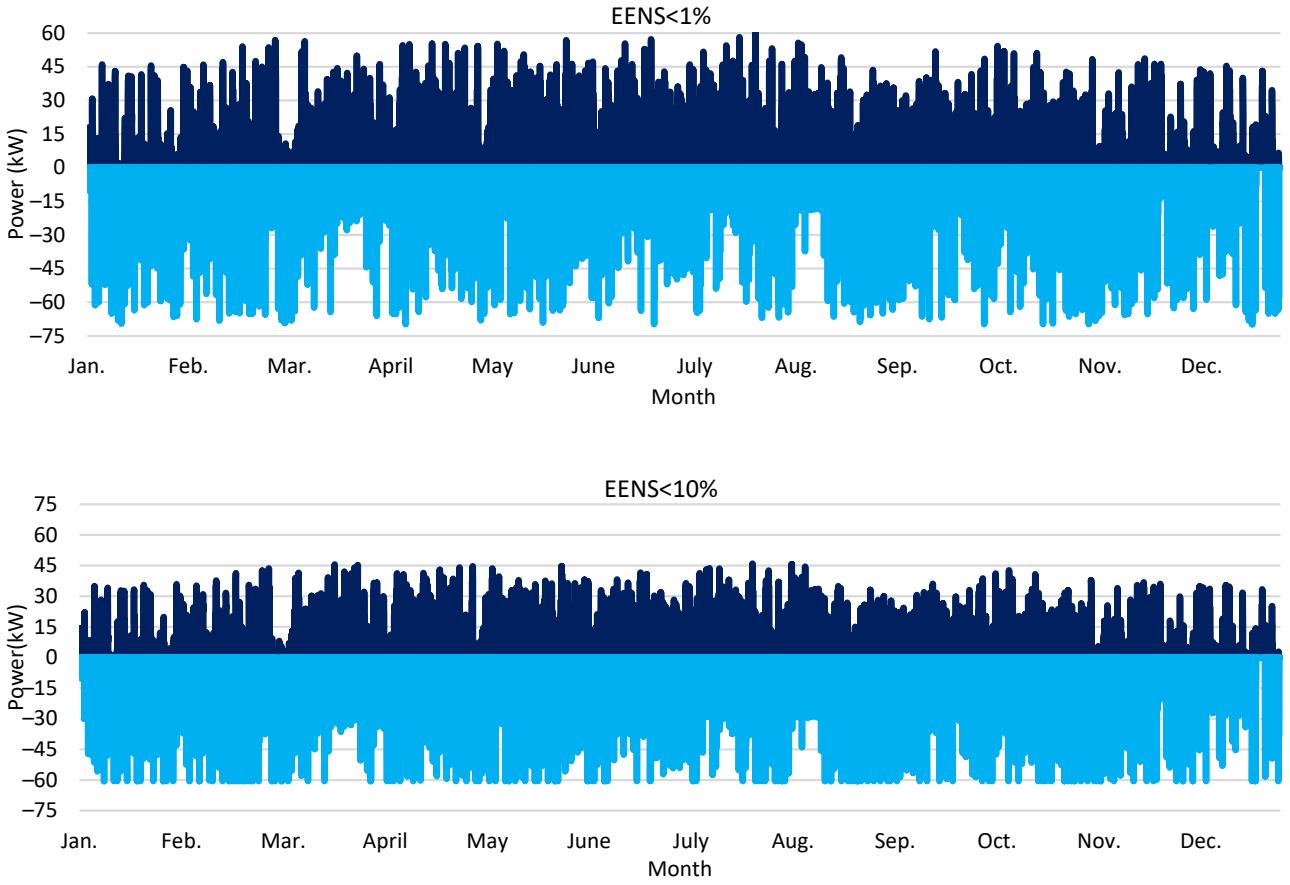

Figure 6. BESS power charge (positive values)/discharge (negative values) for the last year and for two levels of reliability.

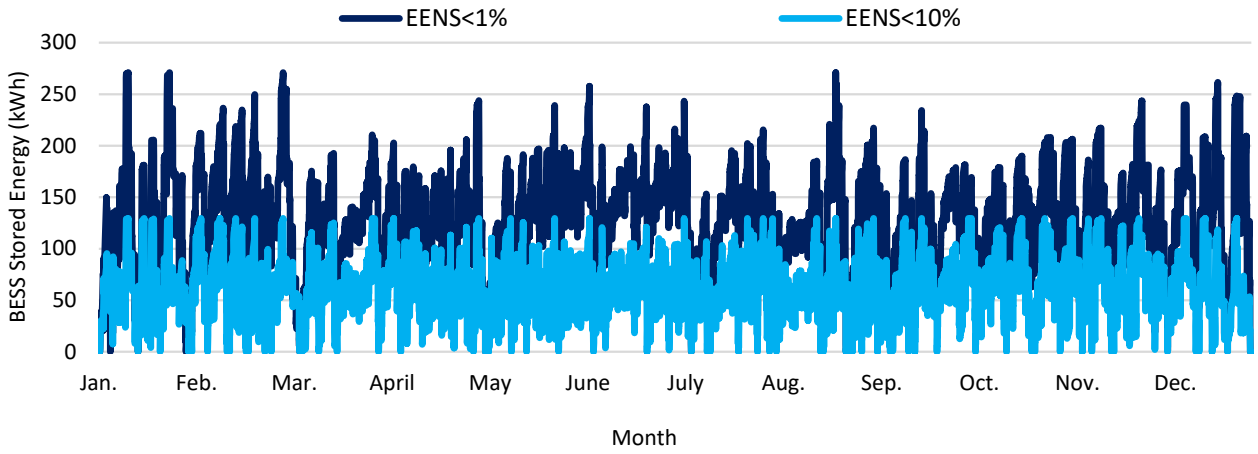

Figure 7. BESS stored energy for two levels of reliability.

To model the higher maintenance cost at the last years of operation, a case study is fulfilled which considers a 10% increase in the OPEX cost for each year and for all components of the system. The results of this case are indicated in Table 1. The results show an increase in the total planning cost due to the 10% yearly increase in the OPEX coefficients. However, the capacity results of each element are the same as when the OPEX coefficients remain constant. This study case and the results are added to the main manuscript.

Table 1. Capacity planning for the study case with variable OPEX.

$EENS_{max}$(%)	Total Cost (GBP)	PV Capacity (kW)	Wind Capacity (kW)	BESS Capacity (kWh)	Converter Size (kW)
1	139,512	58	5.8	273	70
2	122,309	58	4.5	206	68
3	112,691	52	4.2	193	67
4	105,575	52	2.8	198	67
5	101,117	50	2.8	184	64
6	97,411	51	2.3	171	64
7	94,161	51	2.2	157	61
8	91,186	49	2.3	145	61
9	88,423	49	2.0	142	59
10	85,797	49	1.7	132	59

4.2. Results of the Cost–Benefit Optimisation Scenario without Reliability Constraints

In this section, the results are scrutinised when the profit acquired by charging EVs is taken into account. In order to find the optimal case, in this scenario, the EENS is not constrained. The results are presented for three discount rates of 0, 3%, 5%, and two charging prices including 0.55 GBP/kWh and 0.8 GBP/kWh. Table 2 shows the summary of the results for these case studies.

Table 2. Results of the cost benefit model for various discount rates.

	Charging Price (GBP/kWh)	Total Cost (GBP)	Total Income (GBP)	NPV (GBP)	PV Capacity (kW)	Wind Capacity (kW)	BESS Capacity (kWh)	Total Unmet Load (%)
Discount Rate = 0	0.55	60,556	167,250	71,694	44	0	100.5	13.1
	0.8	72,676	258,118	150,442	44	1.6	115.8	7.8
Discount Rate = 3%	0.55	55,760	136,308	45,548	40.5	0	90.2	15.8
	0.8	66,421	211,036	109,614	43.7	0	109.8	10.3
Discount Rate = 5%	0.55	52,368	119,087	31,718	38.2	0	83	18.1
	0.8	62,671	185,573	87,901	43.1	0	102.6	12

It is clear from this table that when the discount rate increases, not only does the NPV decrease, as expected, but also the proportion of unmet EV load increases. Conversely, when the charging price increases from 0.55 to 0.8 GBP/kWh, the NPV increases, and a higher proportion of the EV load is met. From the NPV values, GBP 35,000 has been subtracted and the figures in this table show the final NPV for each case (sum of the EV charger and CDM costs). Figure 8 shows the amount of unmet load for each year when the discount rate is equal to zero. The amount of unmet load also increases for the other cases during the final years of the project.

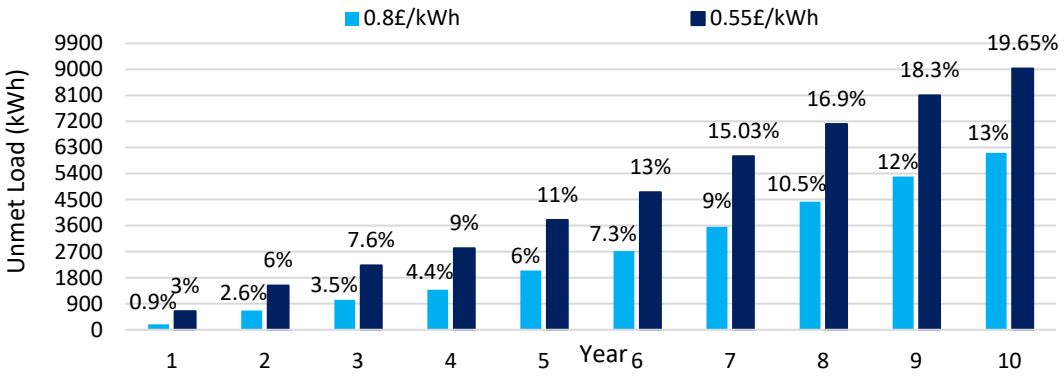

Figure 8. Amount of unmet load for each year for the discount rate of zero for the cost–benefit model and for two different EV charging prices.

4.3. Results of the IGDT Optimisation

This section illustrates the results of the IGDT approach for managing system uncertainties. The method is applied to the unmet load-constrained model. In this study, the results are shown for two strategies including the risk-averse and opportunity-seeking strategy, and for the variations in EV charging load and PV generation.

4.3.1. IGDT Results for the Risk-Averse Strategy

For this strategy, the decision maker is pessimistic about the EV charging load and PV generation. The results for this case are based on a planning cost of GBP 265,891 (risk-neutral), which is for the case with the maximum reliability. It is assumed that the planning budget can be increased to 20% in this case. Figure 9 depicts the variations in the uncertainty budget with the robustness radii of uncertainty for the EV charging load and PV generation, respectively. It is observed that by increasing the planning budget to GBP 319,609, the planning is robust for an increase in the EV charging load up to 20% and the decrease in PV generation of 21.3% for all the planning hours in the worst case. Or, the left figure shows that if the planning cost increases to GBP 308,000 (assuming a GBP 42,542 increase in the planning cost which will be the uncertainty budget), there can be an increase of 16% in the EV charging load or a decrease of 18% in PV generation assuring 100% reliability for the system. Figure 9 also shows the robustness radius for other uncertainty budgets for the EV charging load and the PV generation.

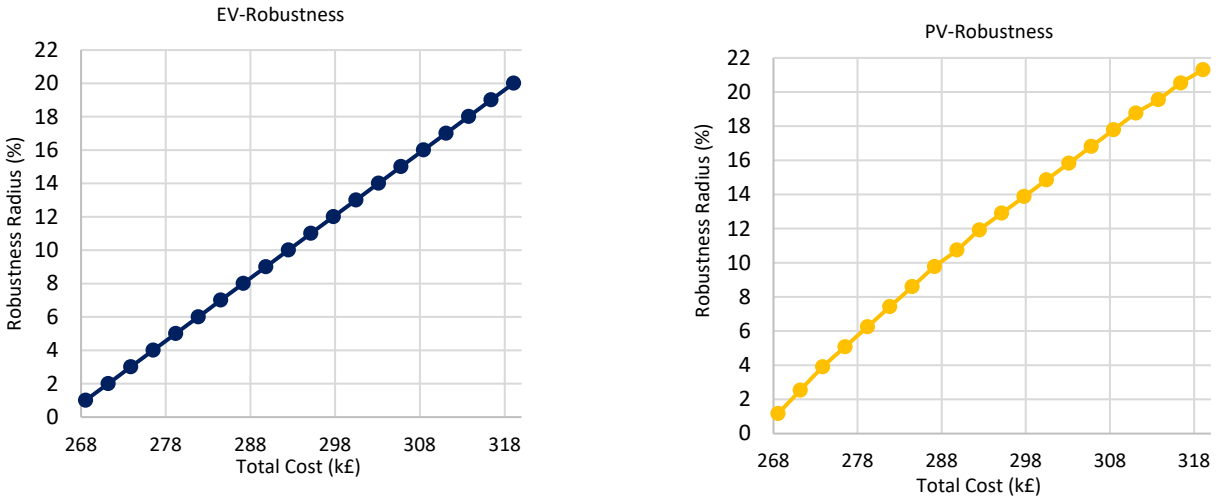

Figure 9. Variation in the robustness radius with the uncertainty budget for EV charging load uncertainty and PV generation uncertainty.

Figure 10 shows the size of the PV generation system and BESS capacity for each amount of uncertainty budget and the cases for EV charging load and PV generation robustness. In these figures, for the EV charging load robustness, the capacities of both the BESS and PV system increase to deal with the maximum increase in the EV charging load restricted by the uncertainty budget. In this case, the BESS and PV system capacities change in the intervals of 405–481 kWh and 236–280 kW, respectively. Furthermore, for the PV generation robustness, while the PV capacity variations are in the interval of 237–297 kW, the BESS capacity remains close to 400 kWh for different values of the uncertainty budget. It is worth mentioning that in these studies, the wind generation capacity is zero for all the cases.

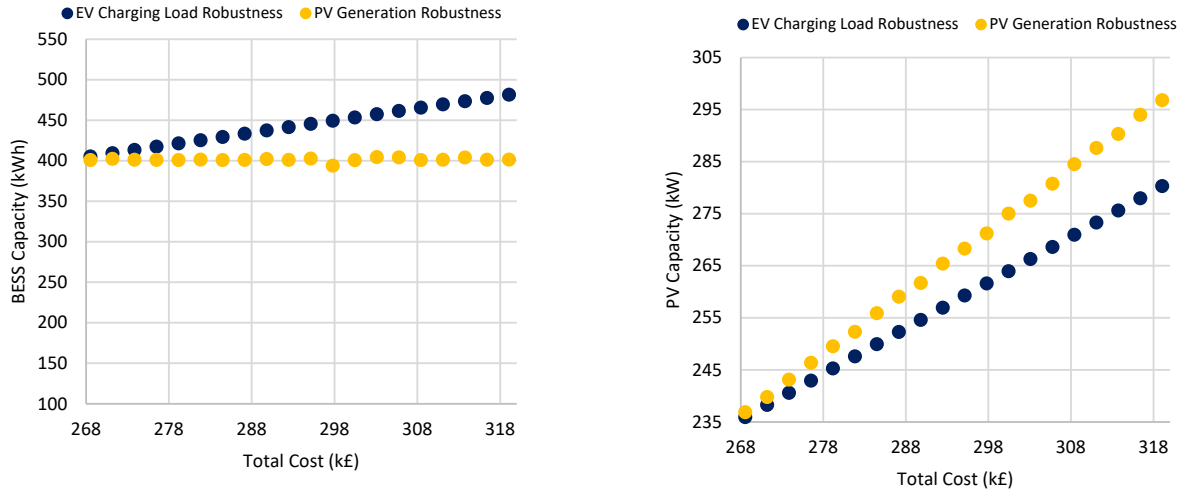

Figure 10. BESS and PV system capacity variations with the total cost for EV charging load and PV generation uncertainty for the risk-averse strategy.

4.3.2. IGDT Results for the Opportunity-Seeking Strategy

In this strategy, the decision maker is optimistic about the EV charging load and PV generation. Figure 11 shows the variation in the opportuneness radius when decreasing the planning cost according to the opportunistic factor for the EV charging load and PV generation. For the EV charging load, it can be seen that if the EV charging load decreases by 20% for the best case for all planning time intervals, the total planning cost of the system will also decrease by 20%. For the PV generation system, the opportuneness radius is about 37.5%. In other words, if the PV generation increases by 37.5% for all planning hours, the total planning cost will decrease by 20%. Or, if the decision maker intends to decrease the total planning cost from GBP 265,891 to GBP 242,000, the EV charging load has to decrease to near 10%, or the PV generation has to increase near to 15%. Like the risk-averse case, the variations for the BESS and PV system capacities are illustrated in Figure 12 for different amounts of total cost specified by the opportunistic factor. This figure shows that for the EV charging load reduction, the battery capacity changes in the range of 320 to 397 kWh and the PV capacity changes from 187 to 231 kW. Also, for the PV generation opportuneness strategy, while the PV capacity changes in the range of 170 to 230 kW, the BESS capacity remains close to 400 kWh for all the opportuneness factors. In other words, for both the risk-averse and opportunity-seeking strategies, only the PV capacity is affected by the robustness and opportuneness radii of uncertainty caused by PV generation.

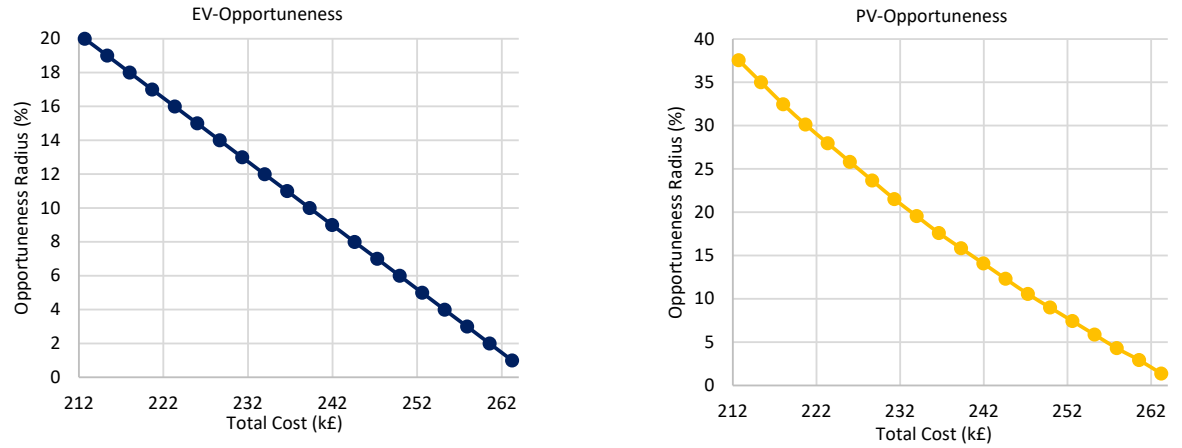

Figure 11. Variation in the opportuneness radius with the total cost for EV charging load and PV generation uncertainty.

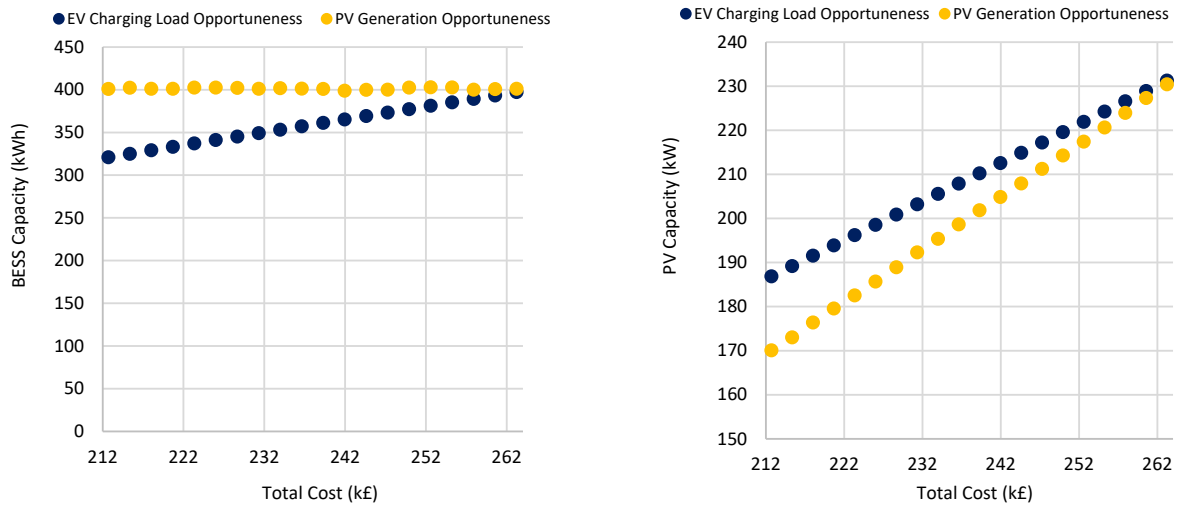

Figure 12. BESS and PV system capacity variations with the total cost for EV charging load and PV generation uncertainty for the opportunity-seeking strategy.

5. Conclusions

This paper presents an optimisation framework for sizing the various components of a stand-alone microgrid for supplying EV charging stations at a visitor attraction site near Southampton, UK, using different levels of reliability. Two different scenarios are studied. In the first one, the CAPEX and OPEX of the project are minimised considering a constraint of the maximum amount of unmet load for each year. In the second scenario, the objective function is based on the NPV of the project without limitation on the amount of unmet load. The results indicate that for the first scenario, the presented framework is able to obtain the optimal size of each component in terms of minimising the CAPEX and OPEX cost for the microgrid and for a certain amount of unmet charging of the EVs at the stations. While supplying 99% of the EVs' demand at the charging station results in a cost of GBP 131,428 for the system, this expenditure decreases to GBP 79,773 if meeting only 90% of the EVs' demand at the charging station is acceptable. For various levels of reliability, higher capacities of PV generation are preferred compared to wind turbines due to the lower investment cost and the nature of diurnal load profile. Moreover, the optimiser plans more BESS capacities when higher levels of reliability are desired instead of increasing the renewable generation capacity.

In the second scenario, the results show that when the amount of the discount rate increases, there are fewer variations in the size of PV systems and wind capacity, but the BESS capacity variations are considerable. The results also show that the amount of unmet load increases with the increase in the discount rate. The EV charging price is another important factor in this study; when it increases, not only does the NPV increase but also the amount of unmet load decreases, which is caused by increasing the size of the PV generation system and BESS capacities.

In the uncertainty studies, the information gap decision theory (IGDT) is used to manage the uncertainties according to risk-averse and opportunity-seeking strategies. For the risk-averse strategy, the results show that by increasing the uncertainty budget up to 20%, the system is able to handle a 20% increase in the EV charging load and a 21.3% in PV generation reduction. For the opportunity-seeking strategy, the results also indicate that the total planning cost can be decreased up to 20% for an EV charging load reduction of 20% or a PV generation increase of 37.5%. The results also show that for the case of PV generation variations, the battery capacity does not change, and the uncertainty is managed by changing the PV capacity.

The core findings of the paper can be summarised as follows:

- For the first scenario, the optimiser prefers to size PV panels and battery energy storage systems rather than wind turbines due to the diurnal EV charging load profile and the CAPEX of the components.
- When higher levels of reliability are desired for the system from 10 to 3%, the optimiser increases the size of the battery, and the PV generation size is almost constant. For reliability levels more than 3%, both the PV generation capacity and battery size increase.
- For the second scenario, when the discount rate increases, only the size of the BESS changes. Also, by increasing the charging price, in addition to the NPV, the sizes of the PV system and BESS increase, which results in decreasing the unmet load.
- For the IGDT studies, the results show that for the EV load charging variations, both the PV generation and BESS capacity change for both the RA and OS strategies. However, for the case of PV generation, the optimiser manages the uncertainty by only changing the capacity of the PV panels and keeping the BESS capacity constant.

Future work can be focused on the concurrent planning of EV charging stations supplied by microgrids and the cyber-security of these systems. Microgrids are becoming more digitised and more dependent on information and communication technology (ICT). Therefore, in order to assure the security of these systems against cyber vulnerabilities, automated control systems which are able to predict, detect, and protect microgrids against cyber-attacks will be needed.

Another possible future research can consider hybrid BESSs composed of different technologies to take advantage of their different features.

Author Contributions: Conceptualization, A.K., Y.A.-W., E.J.F., S.M.S. and A.J.C.; Methodology, A.K.; Software, A.K.; Validation, A.K. and A.J.C.; Formal analysis, A.K., S.M.S., R.G.W., D.A.S. and A.J.C.; Investigation, A.K., D.A.S. and A.J.C.; Data curation, Y.A.-W., E.J.F. and M.N.; Writing—original draft, A.K.; Writing—review & editing, Y.A.-W., E.J.F., M.N., M.J.S., S.M.S., R.G.W., D.T.G., D.A.S. and A.J.C.; Supervision, S.M.S., R.G.W., D.T.G., D.A.S. and A.J.C.; Project administration, S.M.S. and A.J.C.; Funding acquisition, A.J.C. All authors have read and agreed to the published version of the manuscript.

Funding: The authors acknowledge the financial support received from the Engineering and Physical Sciences Research Council (EPSRC) through the 'Future Electric Vehicle Energy networks supporting Renewables' (FEVER) grant, EP/W005883/1.

Data Availability Statement: The datasets presented in this article are not readily available because the data are part of an ongoing study. Requests to access the datasets should be directed to the authors.

Conflicts of Interest: The authors declare no conflict of interest.

Nomenclature

Sets and indices

t	Index for set of time
y	Index for set of year
N_T	Total time intervals for one year
N_Y	Total number of years
PV	Index for PV generation
W	Index for wind generation
BESS	Indices for battery
ch	Battery charge
dis	Battery Discharge
$Conv$	Index for converter
RA	Risk averse strategy
OS	Opportunity seeking strategy

Parameters	
$CAPEX$	Capital cost of system (GBP/kW) or (GBP/kWh)
$OPEX_{,F}$	Fixed operation and maintenance cost (GBP/y)
$OPEX_{,V}$	Variable operation and maintenance cost (GBP/kWh/y)
Δt	Time interval (h)
$Wind$	Wind generation (kW) for 1 kW installed capacity
PV	PV generation (kW) for 1 kW installed capacity
$C_{,max}$	Maximum capacity of each element (kW) or (kWh)
M	Large value
η	Efficiency
EV	Electric vehicle charger load (kW)
r	Discount rate
Pr_{EV}	EV charging cost (GBP/kWh)
Variables	
C	Power of component (kW) or (kWh)
P	Power of component (kW)
UL	Unmet load (kWh)
RS	Renewable spillage (kWh)
u	Binary variable indicating operation mode of battery
E	Battery stored energy (kWh)
$EENS$	Expected energy not supplied

References

1. Mondejar, M.E.; Avtar, R.; Diaz, H.L.B.; Dubey, R.K.; Esteban, J.; Gómez-Morales, A.; Hallam, B.; Mbungu, N.T.; Okolo, C.C.; Prasad, K.A.; et al. Digitalization to achieve sustainable development goals: Steps towards a smart green planet. *Sci. Total Environ.* **2021**, *794*, 148539. [CrossRef] [PubMed]
2. Shabaan, M.S.; Mohamed, S.; Ismail, M.; Qaraqe, K.A.; Serpedin, E. Joint planning of smart EV charging stations and DG eco-friendly remote hybrid microgrids. *IEEE Trans. Smart Grid* **2019**, *10*, 5819–5830. [CrossRef]
3. Lotfi, H.; Khodaei, A. AC versus DC microgrid planning. *IEEE Trans. Smart Grid* **2015**, *8*, 296–304. [CrossRef]
4. Khazali, A.; Al-Wreikat, Y.; Fraser, E.; Naderi, M.; Smith, M.; Sharkh, S.; Wills, R.; Gladwin, D.; Stone, D.; Cruden, A. Sizing a renewable-based microgrid to supply and electric vehicle charging station: A design and modelling approach. In Proceedings of the 37th International Electric Vehicle Symposium & Exhibition, Seoul, Republic of Korea, 23–26 April 2024.
5. Bandyopadhyay, S.; Mouli, G.R.C.; Qin, Z.; Elizondo, L.R.; Bauer, P. Techno-economical model-based optimal sizing of PV-Battery systems for microgrids. *IEEE Trans. Sustain. Energy* **2019**, *11*, 1657–1668. [CrossRef]
6. Khezri, R.; Mahmoudi, A.; Haque, M.H. A demand side management approach for optimal sizing of standalone renewable battery systems. *IEEE Trans. Sustain. Energy* **2021**, *12*, 2184–2194. [CrossRef]
7. Nguyen, T.A.; Crow, M.L.; Elmore, A.C. Optimal sizing of a Vanadium redox battery system for microgrid systems. *IEEE Trans. Sustain. Energy* **2015**, *6*, 729–737. [CrossRef]
8. Alharbi, H.; Bhattacharya, K. Stochastic optimal planning of battery energy storage systems for isolated microgrids. *IEEE Trans. Sustain. Energy* **2017**, *9*, 211–227. [CrossRef]
9. Ren, H.K.; Ashtine, M.; McCulloch, M.; Wallom, D. An analytical method for sizing energy storage in microgrid systems to maximize renewable consumption and minimize unused storage capacity. *J. Energy Storage* **2023**, *68*, 107735. [CrossRef]
10. Amini, M.; Khorsandi, A.; Vahidi, B.; Hosseinian, S.H. Optimal sizing of battery energy storage in a microgrid considering capacity degradation and replacement year. *Electr. Power Syst. Res.* **2021**, *195*, 107170. [CrossRef]
11. Fallahifar, R.; Kalantar, M. Optimal planning of lithium-ion battery energy storage for microgrid applications: Considering capacity degradation. *J. Energy Storage* **2023**, *57*, 106103. [CrossRef]
12. Habib, S.; Ahmrinejad, A.; Jia, Y. A stochastic model for microgrids planning considering smart prosumers, electric vehicles and energy storages. *J. Energy Storage* **2023**, *70*, 107962. [CrossRef]
13. Chen, X.; Dong, W.; Yang, Q. Robust optimal capacity planning of grid-connected microgrid considering energy management under multi-dimensional uncertainties. *Appl. Energy* **2022**, *323*, 119642. [CrossRef]
14. Tao, Y.; Qiu, J.; Lai, S.; Zhao, J. Adaptive integrated planning of electricity networks and fast charging stations under electric vehicle diffusion. *IEEE Trans. Power Syst.* **2022**, *38*, 499–513. [CrossRef]
15. Guzel, I.; Gol, M. Plug-in electric vehicle load modelling for charging scheduling strategies in microgrids. *Sustain. Energy Grids Netw.* **2022**, *32*, 100819. [CrossRef]
16. Gil-Aguirre, J.; Perez-Londono, S.; Mora-Florez, J. A measurement-based load modeling methodology for electric vehicle fast-charging stations. *Electr. Power Syst. Res.* **2019**, *176*, 105934. [CrossRef]
17. He, C.; Zhu, J.; Lan, J.; Li, S.; Wu, W. Optimal planning of electric vehicle battery centralized charging station based on EV load Forecasting. *IEEE Trans. Ind. Appl.* **2022**, *58*, 6557–6575. [CrossRef]

18. Dai, X.; Wang, Y.; Yang, S.; Zhang, K. IGDT-based economic dispatch considering the uncertainty of wind and demand response. *IET Renew. Power Gen.* **2019**, *13*, 856–866. [CrossRef]
19. Khazali, A.; Rezaei, N.; Ahmadi, A.; Hredzak, B. Information gap decision theory based preventive/corrective voltage control for smart power systems with high wind penetration. *IEEE Trans. Ind. Inform.* **2018**, *14*, 4385–4394. [CrossRef]
20. Rezaei, N.; Ahmadi, A.; Nezhad, A.E.; Khazali, A. Information-Gap Decision Theory: Principles and Fundamentals. In *Robust Optimal Planning and Operation of Electrical Energy Systems*; Mohammadi-ivatloo, B., Nazari-Heris, M., Eds.; Springer: Cham, Switzerland, 2019. [CrossRef]
21. Yao, R.; Xie, H.; Wang, C.; Xu, X. A multi-agent-based microgrid day-ahead optimal operation framework with liquid air energy storage by hybrid IGDT-STA. *J. Energy Storage* **2024**, *86*, 111318. [CrossRef]
22. Tayyab, M.; Hauer, I.; Helm, S. Holistic approach for microgrid planning for e-mobility infrastructure under consideration of long-term uncertainty. *Sustain. Energy Grids Netw.* **2023**, *34*, 101037. [CrossRef]
23. Jordehi, A.R. Information gap decision theory for operation of combined cooling, heat, and power microgrids with battery charging stations. *Sustain. Cities Soc.* **2021**, *74*, 103164. [CrossRef]
24. Sun, K.; Li, C.; Peng, Q. Planning of microgrid based on information gap decision theory. In Proceedings of the IEEE 4th Conference on Energy Internet and Energy System Integration (EI2), Wuhan, China, 30 October–1 November 2020.
25. Benheim, Y. *Information Gap Decision Theory, Designs Under Severe Uncertainty*, 2nd ed.; Elsevier Science: San Diego, CA, USA, 2006.
26. Solar Module Phaesun Sun Plus 200_5. Available online: https://order.phaesun.com/en/product/310269.html (accessed on 15 March 2023).
27. Wind-Turbine-Models, Aventa AV-7. 2023. Available online: https://en.wind-turbine-models.com/turbines/1529-aventa-av-7 (accessed on 15 March 2023).
28. Naderi, M.; Palmer, D.; Smith, M.J.; Ballantyne, E.E.F.; Stone, D.A.; Foster, M.P.; Gladwin, D.T.; Khazali, A.; Al-Wreikat, Y.; Cruden, A.; et al. Techno-economic planning of a fully renewable energy-based autonomous microgrid with both single and hybrid energy storage systems. *Energies* **2024**, *17*, 788. [CrossRef]
29. BloombergNEF, Top 10 Energy Storage Trends in 2023. 2023. Available online: https://about.bnef.com/blog/top-10-energystorage-trends-in-2023/ (accessed on 15 March 2023).
30. Gurobi Optimization, LLC. Gurobi Optimizer Reference Manual. 2023. Available online: https://www.gurobi.com/ (accessed on 15 March 2023).
31. FEVER, Future Electric Vehicle Energy Netwoks Supporting Renewables. Available online: https://www.fever-ev.ac.uk/ (accessed on 15 March 2023).